Int J Clin Exp Med 2017;10(5):7597-7610
www.ijcem.com /ISSN:1940-5901/IJCEM0050573

Original Article

Metabolic profiling: shedding new light on the pathophysiological process and prognosis of HBV-related acute-on-chronic liver failure

Liujuan Ji[1*], Xia Liu[2*], Yu Liu[1], Hui Zhu[1], Yuyi Zhang[1], Zhengguo Zhang[1], Hongying Guo[1], Wei Yuan[1], Zhiping Qian[1], Naixia Zhang[2], Jiefei Wang[1]

[1]*Department of Liver Intensive Care Unit, Shanghai Public Health Clinical Center, Fudan University, Shanghai 201508, P. R. China;* [2]*CAS Key Laboratory of Receptor Research, Department of Analytical Chemistry, Shanghai Institute of Materia Medica, Chinese Academy of Sciences, Shanghai 201203, P. R. China.* [*]*Equal contributors.*

Received February 10, 2017; Accepted March 16, 2017; Epub May 15, 2017; Published May 30, 2017

Abstract: Severe global metabolic deterioration is a key feature of hepatitis B virus-related acute-on-chronic liver failure (HBV-ACLF). To investigate the global metabolic changes of HBV-ACLF patients and explore the prognostic potential, extracted metabolic profiling information will shed new light on the pathophysiological process and prognosis of this disease. An NMR-based metabolomics study and its coupled survival prediction ability analysis were applied to the serum samples of healthy controls (HC, n=23), chronic hepatitis B patients (CHB, n=27), surviving HBV-ACLF patients (ACLF-S, n=24) and non-surviving HBV-ACLF patients (ACLF-NS, n=30). The score plots from the metabolomics analysis reveal clear metabolic separations of the HBV-ACLF patients from the CHB individuals and of the surviving HBV-ACLF individuals from the non-surviving ones. Ultimately, 14 discriminative metabolites, including lipids, LDL and twelve amino acids, presented consecutive changes with the progression of HBV-ACLF. These metabolites potentially play important roles in the progression of HBV-ACLF. The averaged sensitivity and specificity values of the survival prediction models based on metabolomics data are 76.7% and 83.3%, respectively. The combined use of metabolomics data and clinical parameters raises the sensitivity and specificity values of the predicted score plot up to 91.7% and 90%, respectively. The phenotypic metabolomics analyses of HC, CHB, ACLF, ACLF-S and ACLF-NS individuals provides an encouraging basis for deeper studies of the HBV-ACLF pathophysiological process and demonstrates a proof of concept that global metabolic profiling data is a reliable source to improve the accuracy of predicting the survival outcome of HBV-ACLF patients.

Keywords: Metabolic profiling, HBV, ACLF, outcome prediction, discriminative metabolite

Introduction

Hepatitis B virus-related acute-on-chronic liver failure (HBV-ACLF) is one of the most dangerous end-stage liver diseases, with varied clinical manifestations and extremely poor prognosis caused by progressive multiple organ failure [1, 2]. Due to the rapid progress of the disease and the less robust treatment options, the mortality rate of ACLF patients is as high as 50-90% [1, 3]. To ameliorate the situation, extensive effort needs to be put into the HBV-ACLF disease field, including pathophysiological studies, the development of novel therapeutic methods and the exploration approach for the assessment of early prognosis. The achievements obtained through pathophysiological studies of HBV-ACLF will provide a strong basis for the development of novel treatments of this disease. Meanwhile, with the help of the reliable early prognostic assessment, clinicians could separate patients with irreversible deterioration, leaving liver transplantation as the only realistic therapeutic option, from those individuals who will fully recover with only intensive supportive care. It is worth noting that the best way to evaluate the severity and prognosis of HBV-ACLF patients with a high sensitivity and specificity remains a big concern worldwide. In practice, the Child-Turcotte-Pugh (CTP) score [4] and the Model for End-Stage Liver Disease (MELD) score [5, 6] are two commonly used parameters for the evaluation of the prognosis of cirrhosis patients. In addition, the Chronic

Liver Failure-Sequential Organ Failure Assessment (CLIF-SOFA) score [7] is a newly developed scoring system for patients with end-stage liver disease. To evaluate the prognosis of HBV-ACLF, the sensitivity and specificity of these currently used prognostic approaches are debatable because none of them was established using data from HBV-ACLF patients or taking into account the metabolic perturbations determined by liver diseases.

The liver is the primary organ of metabolism in the human body, and HBV-ACLF will inevitably cause perturbations of multiple metabolic pathways. In fact, severe global metabolic deterioration is a key feature of HBV-ACLF [8]. Therefore, to investigate the global metabolic profile changes of HBV-ACLF patients, using a metabolomics approach will provide an encouraging basis for deeper studies of the pathophysiological process of this disease. Additionally, the extracted metabolic profiling information could potentially serve as a complementary method for the assessment of the early prognosis of HBV-ACLF patients. Metabolomics, which measures the metabolic profiles in biological samples, such as isolated cells, tissues or biofluids, using multivariate analysis techniques and accurately reflects the global metabolic status of biological systems, has become a promising and powerful technique for toxicity assessment, disease diagnosis and prognosis judgment [9]. In recent years, metabolomics has been increasingly applied to identify the biomarkers in various liver diseases, including drug-induced liver injury [10], autoimmune hepatitis (AIH) [11], viral hepatitis [12], cirrhosis [13, 14], hepatic encephalopathy [14], and acute and chronic liver failure [15]. Moreover, quite a few promising findings have been reported. Amathieu *et al.* [16] found that the severity of chronic liver failure is well correlated with the impairments of lipid, glucose and amino acid metabolism. Saxena *et al.* [17] reported that a single biomarker (Glutamine) could predict an unfavorable outcome with a high sensitivity in fulminant hepatic failure cases. However, the application of a metabolomics approach in the ACLF/HBV-ACLF research field has been rather limited. Specially, no metabolomics study has been performed to investigate the discriminative metabolic signatures of surviving and non-surviving HBV-ACLF patients. Therefore, to extract the global metabolic profile information of HBV-ACLF patients, here in this paper, a systematic ^{1}H NMR-based metabolomics study was applied to the serum samples of healthy control individuals (HC), chronic hepatitis B patients (CHB), the surviving HBV-ACLF patients (ACLF-S) and the non-surviving HBV-ACLF patients (ACLF-NS). The metabolic profile differences of the four groups were then determined. The multivariate statistical models for assessing the severity and predicting the clinical outcomes of HBV-ACLF individuals were also established. The averaged sensitivity and specificity of the survival prediction models were determined to be 76.7% and 83.3%, respectively, which indicated an acceptable prediction capability of the extracted metabolic profile data. Specifically, when used in combination with clinical parameters, the sensitivity and specificity of the predicted score plots reached encouraging values of 91.7% and 90%, respectively. Our findings provide a great basis for further pathophysiological studies of HBV-ACLF and a potential complementary method for the prognosis of this disease.

Materials and methods

Ethics statement

This research project was performed in accordance with the principles of the Helsinki Declaration II and approved by the Human Ethics Committees of the Shanghai Public Health Clinical Center, Fudan University. All of the participants or their guardians provided written informed consent for participation in the research project.

Patients and sample collection

Four cohorts of 54 patients with HBV-ACLF (including 24 surviving patients (ACLF-S subgroup) and 30 non-surviving individuals (ACLF-NS subgroup)), 27 chronic hepatitis B patients (CHB), and 23 age- and sex-matched healthy controls (HC) were recruited at the Shanghai Public Health Clinical Center. Patients were diagnosed with ACLF by following the "Diagnostic and Treatment Guidelines for Liver Failure" in China [18]. The diagnostic criteria include HBsAg-positive or HBV DNA-positive for more than 6 months, acute hepatic insult manifesting as jaundice and coagulopathy, prothrombin activity (PTA) $\leq$ 40% (or international normalized ratio (INR) $\geq$ 1.50), and serum total

bilirubin (TBIL) ≥ 10 mg/dL or a daily elevation ≥ 1 mg/dL. HBV-ACLF individuals with hepatitis virus (A, C, D, E) infection, human immunodeficiency virus (HIV) infection, hepatocellular carcinoma, any other types of cancer, autoimmune diseases, kidney diseases, hematological diseases, diabetes or hyperthyroidism, and peritonitis or other severe infection were excluded from this project. All healthy volunteers with no prior history of liver disease were recruited from the medical examination center of Shanghai Public Health Clinical Center, and the age, gender, and biochemical characteristics of these volunteers were recorded.

All the HBV-ACLF patients were followed up for at least 90 days after hospital admission. According to the 90-day clinical outcomes, patients with HBV-ACLF were further divided into the survival (n=24) (with remarkably improved clinical symptoms, physical signs and liver function (TBIL < 5 times of the normal upper limit, PTA > 40% or INR < 1.50)) and the non-survival subgroups (n=30). Additionally, none of these surviving patients underwent liver transplantation. All blood samples were obtained between March 2015 and January 2016 from recruited patients at Shanghai Public Health Clinical Center. Five milliliters of venous peripheral blood were extracted under fasting conditions within 24 hours of admission to the hospital into ethylenediaminetetraacetic acid (EDTA) tubes and centrifuged at 12,000 g for 10 min at 4°C within 1 hour after sample collection. The supernatant (300 μL) was aliquoted in 1.5 mL Eppendorf tubes and then stored at -80°C prior to analysis.

^{1}H NMR spectroscopy

For NMR analysis, frozen plasma samples were thawed at room temperature. An aliquot of plasma (300 μL) was added to 300 μL of 0.2 M phosphate buffer (Na_2HPO_4/NaH_2PO_4, pH 7.4) and centrifuged at 12,000 g for 10 min at 4°C. Samples of supernatant (500 μL) were moved into 5 mm NMR tubes and then 50 μL of D2O containing 0.01% sodium 3-(trimethylsilyl) [2, 2, 3, 3-D4] propionate (TSP) was added.

NMR spectra were acquired in a random, blinded order on a Bruker (Karlsruhe, Germany) Avance™ III 600 MHz spectrometer (Bruker GmbH, Rheinstetten, Germany) equipped with a cryoprobe operating at 600.13 MHz and 25°C. The free induced decays (FID) were acquired using Carr-Purcell-Meiboom-Gill (CPMG) spin echo sequence to attenuate the broader peaks arising from proteins and lipids. A standard pulse sequence (relaxation delay-90°-(τ-180°-τ)$_n$-acquire FID) was employed, and the water resonance was pre-saturated during the relaxation delay (4 s). A fixed total spin-spin relaxation delay (2 nτ) of 120 ms was taken to measure spin-echo ^{1}H spectra. For each sample, 256 transients were recorded into 32 K data points over a spectral width of 64 kHz with an acquisition time of 2.73 s.

Data processing for statistical analyses

FID processing was performed using the software MestReNova Version 8.1.4 (Mestrelab Research S.L.). Fourier transformation was performed with the exponential weighting factor of a 0.3 Hz line-broadening factor and a zero filing factor of 2 to improve the signal-to-noise ratio of the spectra. Each spectrum was manually phased, baseline-corrected, and carefully aligned. Then, all the 1D NMR spectra were referenced to the methyl group of TSP at 0.00 ppm. The spectral region of δ 9.50-0.50 was segmented into 3000 bins, with a 0.003 ppm width for each one. The integrals of the region of δ 6.50-4.60, with a residual water peak, and the regions of δ 2.53-2.61, δ 2.73-2.68, δ 3.07-3.24, δ 3.59-3.65, with EDTA peaks, were excluded from the analysis. The remaining integrals were normalized to 1. Then, the well-processed data were imported into SIMCA-P software (Version 14.0, Umetrics AB, Umea, Sweden) for multivariate pattern recognition analyses. Principal component analysis (PCA) was first performed to detect any group separation based on NMR signal variability and to identify outliers. Subsequently, the normalized integral values were mean-centered for orthogonal partial least-squares discriminant analyses (OPLS-DA). OPLS-DA was illustrated with the first predictive (t [1]) and one orthogonal component (to [1]). The terms R2X, R2Y, and Q2 were used to evaluate the quality of the OPLS-DA models. R2X and R2Y were the respective fractions of X and Y variance in the data explained by the model and indicated goodness of fit. Q2 represents the cross-validated explained variation and indicated predictability. The standard 7-round cross validation and permutation test (200 cycles) was carried out to measure the robustness of the model.

Table 1. Clinical characteristics of patients with liver diseases (mean ± SD)

Biochemical characteristics	ACLF			CHB	*P* value
	Total	Survivors	Non-survivors		
No. of patients	54	24	30	27	/
Age (years)	42.87±10.03	37.88±7.51	46.87±10.09	39.11±10.64	0.00
Gender (M/F)	45/9	20/4	25/5	20/7	/
ALT (U/L)	372.76±534.31	506.5±771.65	330.53±455.41	46.96±45.08	0.49
AST (U/L)	83.56±294.80	360.83±462.38	259.16±232.10	33.78±18.59	0.47
AKP (U/L)	140.21±44.35	110.33±31.89	150.17±44.08	100.96±21.83	0.05
GGT (U/L)	71.42±34.21	80.17±27.02	68.50±36.50	57.15±42.59	0.48
CHE (U/L)	3668.30±2340.40	3774.38±1854.72	3583.43±2695.47	7730.87±1383.84	0.77
TBIL (μmol/L)	424.16±208.06	270.78±136.30	472.60±205.52	13.46±3.88	0.04
Alb (g/L)	33.53±23.80	40.79±19.09	31.24±25.12	44.70±3.01	0.43
PAB (mg/L)	33.53±23.80	40.79±19.09	31.24±25.12	210.07±37.79	0.40
INR	2.76±1.67	1.61±0.22	3.21±1.78	1.16±0.12	0.02
PTA (%)	33.56±10.95	38.43±8.63	29.67±11.17	83.25±9.62	0.00
PT (s)	28.4±12.91	19.33±3.47	31.26±13.52	13.87±1.36	0.05
Cr (μmol/L)	74.71±34.38	57.22±12.24	80.23±37.41	63.65±10.80	0.16
Glc (mmol/L)	4.76±1.57	5.61±1.95	4.47±1.36	5.44±1.36	0.13
AFP (ng/ml)	111.38±250.11	61.02±58.90	124.63±279.77	6.27±8.75	0.62
Lactate (mmol/L)	2.31±1.71	1.92±0.49	2.44±1.96	/	0.53
Ammonia (μmol/L)	99.64±40.35	71.5±15.16	108.53±41.94	/	0.05
CRP (mg/L)	13.15±13.42	23.48±26.97	10.43±5.55	/	0.05
HGB (g/L)	109.05±14.72	108±12.12	109.24±15.45	146.69±11.53	0.90
WCC (×109)	7.42±3.27	7.65±3.56	7.35±3.28	5.30±1.59	0.85
PLT (×109)	103.36±55.36	96.67±39.66	105.47±60.24	143.04±37.02	0.74
Sodium (mmol/L)	136.04±4.38	137.47±0.90	135.59±4.95	140.42±3.58	0.37
Potassium (mmol/L)	3.88±0.57	3.79±0.47	3.91±0.61	4.02±0.32	0.66
ACLF grade (0/1/2/3)	/	41/7/4/2	21/3/0/0	20/4/4/2	0.02
CLIF-SOFA	/	6.56±1.38	6.08±1.21	6.93±1.41	0.02
MELD score	24.63±7.01	20.45±3.82	27.96±7.23	/	0.00

ALT: alanine aminotransferase; AST: aspartate aminotransferase; AKP: alkaline phosphatase; GGT: gamma glutamyltransferase; CHE: cholinesterase; TBIL: total bilirubin; Alb: albumin; PAB: prealbumin; INR, International Normalized Ratio; PTA: prothrombin activity; PT: prothrombin time; Cr: Creatinine; Glc: glucose; AFP: alpha fetal protein; CRP: C-reactive protein; HGB: hemoglobin; WCC: white cell count; PLT: platelet; CLIF-SOFA: Chronic Liver Failure-Sequential Organ Failure Assessment); MELD: Model for End-Stage Liver Disease.

Variable importance in the projection (VIP) derived from the OPLS-DA model ranked the importance of each variable for the classification, and those variables with VIP > 1.0 were initially considered statistically significant in this model. The correlation coefficients (r) of the variables relative to the first model score value in the OPLS-DA model were also extracted from S-plot calculated by Pearson correlation. Cutoff values of r with a significance level of 0.05 were used to identify variables that were responsible for the discrimination of groups. Thus, the integrals of metabolites that had a VIP > 1 and the correlation coefficients |r| > the critical value when P=0.05 accounted for the detected discrimination. The ROC curve plot of each statistically significant metabolite between groups was illustrated to validate their discriminative potential.

Quantitative comparison of metabolites in ^{1}H NMR spectra of serum samples

The average changes of metabolites between the CHB vs. HC, ACLF vs. CHB, and ACLF-S vs. ACLF-NS groups were calculated. Bar graphs were used to depict the variations in the integrals of the statistically significant metabolites in HC, CHB, ACLF, ACLF-S, and ACLF-NS groups. Significant differences in the mean values were

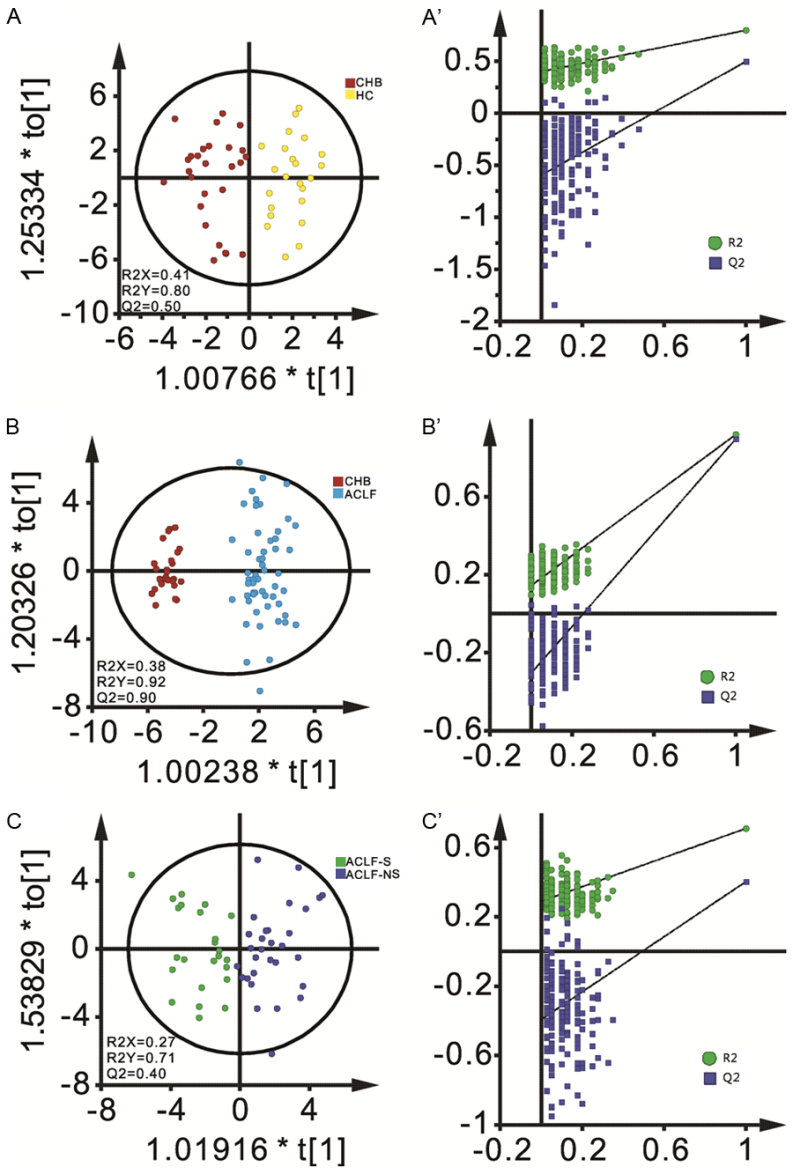

Figure 1. The OPLS-DA score plots (left panel) and permutation tests (right panel) with the 7-round cross-validation of the 1H NMR spectra derived from the serum samples in groups of (A, A') CHB (■) vs. HC (■), (B, B') CHB (■) vs. ACLF (■), (C, C') ACLF-S (■) vs. ACLF-NS (■).

evaluated by a one-way analysis of variance (ANOVA), followed by Bonferroni's or Turkey's post hoc analysis when appropriate. Statistical significance was considered as $P \leq 0.05$. All the statistical analyses were performed using SPSS software (version 17.0, SPSS, Chicago, IL).

The predicative OPLS-DA models for the prognosis of ACLF patients

To evaluate the predictive ability of the OPLS-DA models for non-classified samples (the predictive sets defined by randomly picking one-third of the total samples in each group), the first predictive component was used as the boundary, and the distribution of non-classified samples was observed in the OPLS-DA score plots. The sensitivities of the models were calculated from the ratio between the true positive and the total number of modeled ACLF spectra, whereas the specificities were determined from the ratio between the true negative and the total number of modeled control spectra. Moreover, the predictive ability of metabolomics data, metabolomics data plus clinical parameters, clinical parameters, MELD scores and CLIF-SOFA scores were also evaluated by the area under the ROC curves (AUROC) plots and the predicted scores plots. The clinical parameters, which were used to achieve the predicted score plots, include the age of the experimental individuals and the levels of alkaline phosphatase (AKP), TBIL, INR, prothrombin activity (PTA), prothrombin time (PT), alpha fetal protein (AFP), ammonia and C-reactive protein (CRP) in their serum.

Results

Clinical parameters

The clinical parameters of patients recruited in this study are shown in **Table 1**. Compared to the survivors of ACLF, the levels of AKP, TBIL, INR, PT, CRP and ammonia were significantly elevated in the non-survivors, and the levels of PTA were reduced. The non-survivors exhibited higher MELD scores; however, no statistically significant differences in other clinical parameters were observed in the survivors and fatal cases on the day of hospital admission.

Table 2. The changing trends of discriminative metabolites between groups

Metabolites	% Average changes (CHB *vs.* HC) (|r|, VIP, *p*-Value) (|r| ≥ 0.270)	% Average changes (ACLF *vs.* CHB) (|r|, VIP, *p*-Value) (|r| ≥ 0.220)	% Average changes (ACLF-NS *vs.* ACLF-S) (|r|, VIP, *p*-Value) (|r| ≥ 0.268)
Succinate	/	+160.8 (0.62, 1.23, 0.00)	/
Betaine	/	+110.4 (0.57, 1.05, 0.00)	+29.7 (0.42, 0.98, 0.01)
Threonine	/	-19.99 (0.43, 0.88, 0.00)	-12.2 (0.47, 1.27, 0.00)
Tyrosine	/	+124.5 (0.77, 1.39, 0.00)	+18.07 (0.41, 0.97, 0.01)
Valine	-7.22 (0.32, 1.21, 0.03)	-37.36 (0.78, 1.46, 0.00)	-21.28 (0.49, 1.25, 0.00)
2-Aminobutyrate	/	-24.46 (0.62, 1.20, 0.00)	-17.27 (0.43, 1.13, 0.01)
3-Methyl-2-oxovalerate	/	/	-17.11 (0.29, 0.98, 0.04)
VLDL	-18.67 (0.31, 1.11, 0.01)	+63.09 (0.27, 1.01, 0.00)	-55.59 (0.62, 1.62, 0.00)
LDL	-28.83 (0.35, 1.24, 0.01)	-37.66 (0.32, 0.99, 0.00)	-57.38 (0.67, 1.74, 0.00)
Asparagine	-10.93 (0.36, 0.96, 0.00)	-28.79 (0.62, 1.23, 0.00)	-10.49 (0.31, 1.10, 0.01)
Citrate	+13.52 (0.48, 1.40, 0.01)	+15.82 (0.24, 0.45, 0.00)	/
Creatine	/	/	+30.69 (0.28, 0.72, 0.02)
Creatinine	/	-16.71 (0.35, 0.75, 0.00)	+10.77 (0.33, 0.79, 0.02)
Cystine	-37.8 (0.70, 1.84, 0.00)	/	/
Dimethylglycine	/	-28.89 (0.60, 1.17, 0.00)	/
Glutamine	+8.05 (0.36, 1.11, 0.03)	+12.90 (0.20, 0.58, 0.01)	+16.95 (0.27, 0.75, 0.02)
Isobutyrate	/	+29.97 (0.38, 0.89, 0.00)	/
Isoleucine	-13.84 (0.56, 1.58, 0.00)	-41.19 (0.77, 1.49, 0.00)	-29.85 (0.63, 1.61, 0.00)
Lactate	/	+47.09 (0.51, 0.93, 0.00)	/
Leucine	-10.32 (0.43, 1.40, 0.00)	-30.01 (0.63, 1.27, 0.00)	-25.28 (0.52, 1.31, 0.00)
Lysine	-6.38 (0.41, 1.38, 0.02)	+15.48 (0.30, 0.60, 0.00)	/
Methionine	+9.62 (0.41, 1.25, 0.00)	+271.4 (0.56, 1.20, 0.00)	+123.7 (0.62, 1.51, 0.00)
N-methylhydantoin	/	-30.12 (0.56, 1.06, 0.00)	/
Phenylalanine	/	+79.19 (0.71, 1.32, 0.00)	+20.35 (041, 1.03, 0.01)
Glycine	/	+12.97 (0.18, 0.59, 0.01)	+17.34 (0.40, 1.02, 0.01)
Alanine	-10.08 (0.36, 0.95, 0.01)	-18.13 (0.45, 0.89, 0.00)	/
Histidine	+11.07 (0.44, 1.34, 0.00)	-12.27 (0.50, 1.04, 0.00)	+9.75 (0.46, 1.16, 0.01)
Glucose	+11.68 (0.41, 1.10, 0.00)	-19.07 (0.37, 0.67, 0.00)	-17.97 (0.41, 0.96, 0.01)
Formate	/	+44.07 (0.32, 0.67, 0.00)	/
Lipid	-29.79 (0.36, 1.27, 0.01)	-70.55 (0.62, 1.20, 0.00)	-51.46 (0.65, 1.67, 0.00)

Metabolic alterations of the CHB and the HBV-ACLF patients

Figure S1 shows the representative spectra of the serum samples of the healthy controls (Figure S1A), CHB patients (Figure S1B), and ACLF patients (Figure S1C and S1D). Visual inspection of the spectra can hardly reveal the different metabolic fingerprint profiles of serum metabolites among groups. The observed metabolites in these four serum spectra included creatinine (Cr), creatine (Cre), citrate (Cit), isobutyrate (IB), lactate (Lac), succinate (Suc), lipid, LDL, VLDL, glucose (Glc), dimethylglycine (DMG), formate (For), 3-Methyl-2-oxovalerate (MOV), N-methylhydantoin (Mhd), and amino acids, including lysine (Lys), alanine (Ala), tyrosine (Tyr), valine (Val), glycine (Gly), glutamine (Gln), cystine (Cys), isoleucine (Ile), leucine (Leu), histidine (His), proline (Pro), threonine (Thr), asparagine (Asn), methionine (Met), phenylalanine (Phe), 2-aminobutyrate (2-AB) and betaine (Bet), which were all summarized in Table S1.

To obtain a comprehensive comparison of metabolic profiles among the groups, PCA analyses with the first two principal components (t [1], t [2]) were employed (Figure S2), which revealed diverse trends among different groups. The

healthy individuals and CHB samples clustered to the left section, the ACLF-S group was more close to the HC and CHB groups than the ACLF-NS samples. However, partial overlaps among groups were also observed in the PCA score plots. To identify the metabolic characteristics of patients, pairwise OPLS-DA analyses were performed. Obvious separations between HC and CHB (**Figure 1A**), CHB and ACLF (**Figure 1B**), and ACLF-S and ACLF-NS (**Figure 1C**), with the confirmation of the cross-validation results of permutation tests (**Figure 1A'**, **1B'**, **1C'**), indicate that significant metabolic alterations occurred during the progression of liver disease.

The VIPs and p(corr) values extracted from the OPLS-DA plot revealed that the global metabolic pool of CHB patients was characterized by high peaks for citrate, glutamine, histidine, methionine, and glucose and decreased excretions of valine, VLDL, LDL, asparagine, cystine, isoleucine, leucine, lysine, alanine, and lipid (**Table 2**). Compared with the CHB group members, in the sera of the hepatitis B-related ACLF patients, the levels of succinate, betaine, tyrosine, VLDL, citrate, glutamine, isobutyrate, lactate, lysine, methionine, phenylalanine, glycine, and formate were significantly elevated, and the levels of lipid, glucose, histidine, alanine, N-methylhydantoin, leucine, isoleucine, dimethylglycine, creatinine, asparagine, LDL, 2-aminobutyrate, valine, and threonine were significantly downregulated.

Compared with the ACLF-S group, in the serum samples of ACLF-NS patients threonine, valine, 2-aminobutyrate, 3-methyl-2-oxovalerate, VLDL, LDL, asparagine, isoleucine, leucine, glucose, and lipid were significantly downregulated, while betaine, tyrosine, creatine, creatinine, glutamine, methionine, phenylalanine, glycine, and histidine were considerably upregulated. All of these abovementioned discriminative metabolites were further validated and confirmed by the AUROC values (**Figure 2**). Additionally, we calculated the average changes of metabolites based on the ^{1}H NMR variables between groups and summarized the data in **Table 2**.

Outcome prediction of ACLF patients by NMR-based metabolomics data

Three predictive OPLS-DA models were produced with two-thirds of the total samples in the survival and the non-survival groups, defined as the training set, and the remaining samples were defined as the prediction set. The predictive results were elucidated in terms of sensitivity and specificity, and the averaged sensitivity and specificity of all three models were 76.6% and 83.3%, respectively (**Figure 3**). To establish a more robust prognostic prediction model, the predictive abilities of metabolomics data only, metabolomics data plus clinical parameters, clinical parameters only, MELD scores only, and CLIF-SOFA scores were evaluated using the AUROC plots and the predicted scores plots (**Figure 4**). In general, the data clearly illustrates that the predicted score plot of the metabolomics data plus the clinical parameters has the best sensitivity (91.7%) and specificity (90%) with the greatest AUROC value of 0.97.

Discussion

As a life-threatening disease, HBV-ACLF induces massive necrosis of hepatocytes and has an extraordinarily high mortality. An early and accurate evaluation of the severity of HBV-ACLF plays a supportive role in optimizing the treatment program, preventing or delaying the progression and reducing the mortality of this disease. In addition to rapidly progressive hepatic failure, severe global metabolic deterioration is another key feature of HBV-ACLF. To explore the global metabolic characteristics of HBV-ACLF disease, the use of a metabolomics approach can shed new light on the pathophysiological process and prognosis of this disease. In this study, ^{1}H NMR-based metabolomics was applied to the serum samples of healthy control individuals, chronic hepatitis B patients, surviving HBV-ACLF patients and non-surviving HBV-ACLF patients. Clear group separations were observed between HC *vs.* CHB, CHB *vs.* ACLF and ACLF-NS *vs.* ACLF-S. Among the identified perturbed metabolites (**Table 2**; **Figure 5**), eight of them (lipid, LDL, glutamine, methionine, valine, asparagine, leucine and isoleucine) presented consecutive changes upon the progression of HBV-ACLF (ACLF *vs.* CHB *vs.* HC). Specifically, the changing tendencies for these metabolites were also observed in the serum samples of ACLF-NS patients vs. ACLF-S individuals. In addition to the eight discriminative metabolites with consecutive changing tendencies, six other metabolites, including betaine, threonine, tyrosine, 2-aminobutyrate, phenylalanine and glycine, also showed consecutive changes after the disease had already occurred

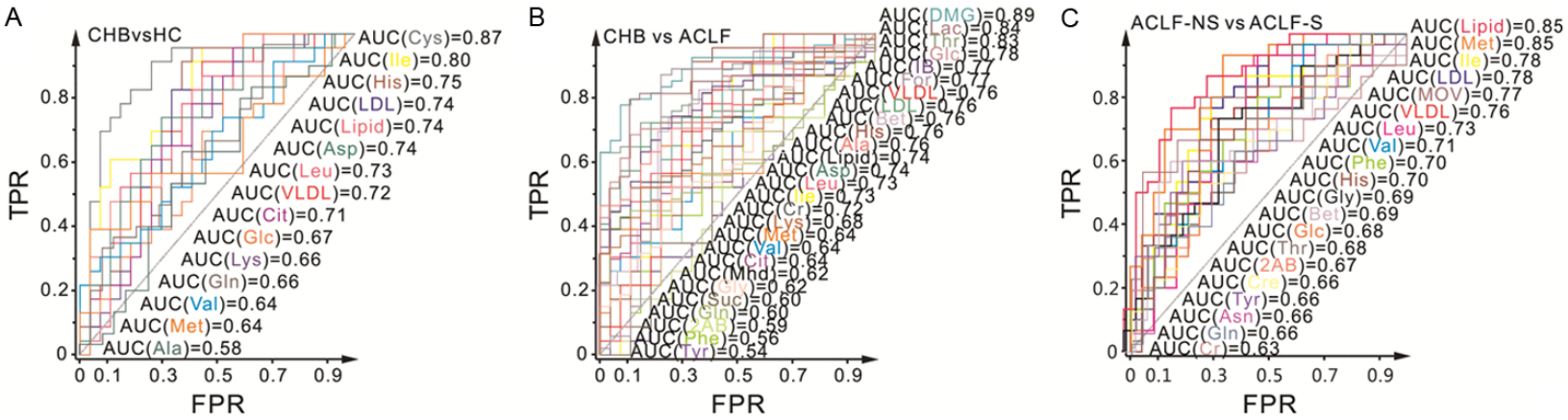

Figure 2. AUROC plots for each discriminative metabolite obtained from the OPLS-DA analyses of **Figure 1**.

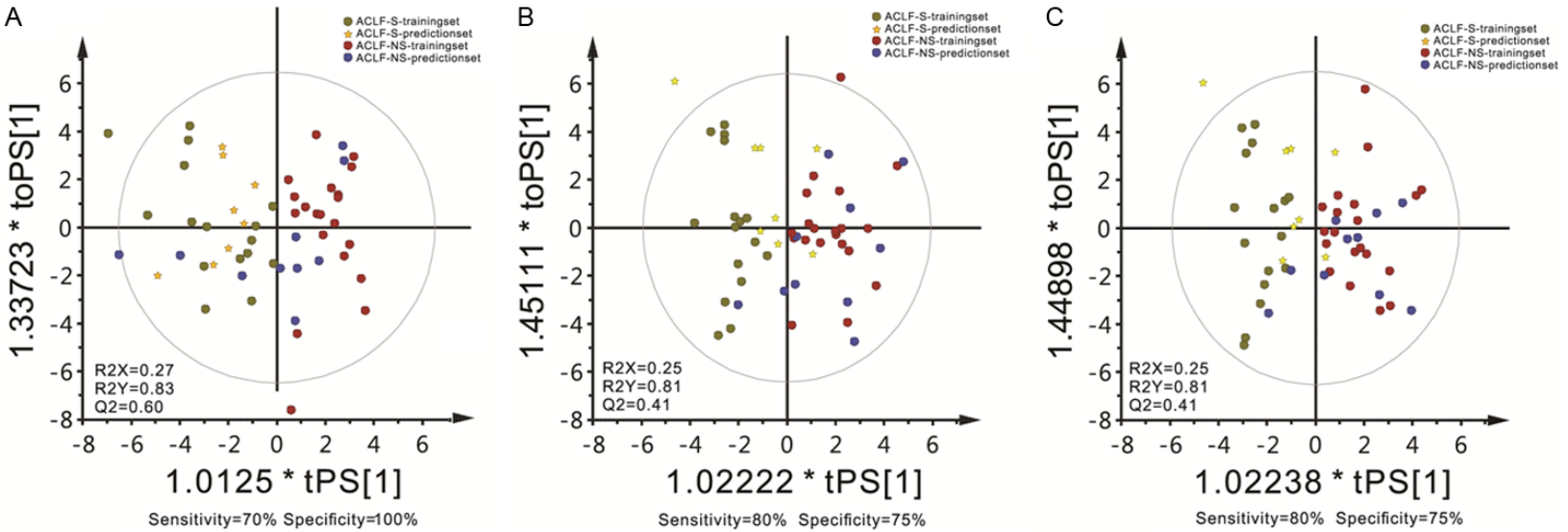

Figure 3. The predictive OPLS-DA models derived from the non-classified predictive sets and the training sets from the ACLF-S and ACLF-NS groups. The training sets used to generate the predictive OPLS-DA models A, B and C were respectively created by randomly picking two-thirds of the total samples from the ACLF-S group and the ACLF-NS group, and the sample compositions for these three training sets were different from each other. A. The sensitivity and specificity of the predictive OPLS-DA model A were 70% and 100%, respectively. B. The sensitivity and specificity of the predictive OPLS-DA model B were 80% and 75%, respectively. C. The sensitivity and specificity of the predictive OPLS-DA model C were 80% and 75%, respectively.

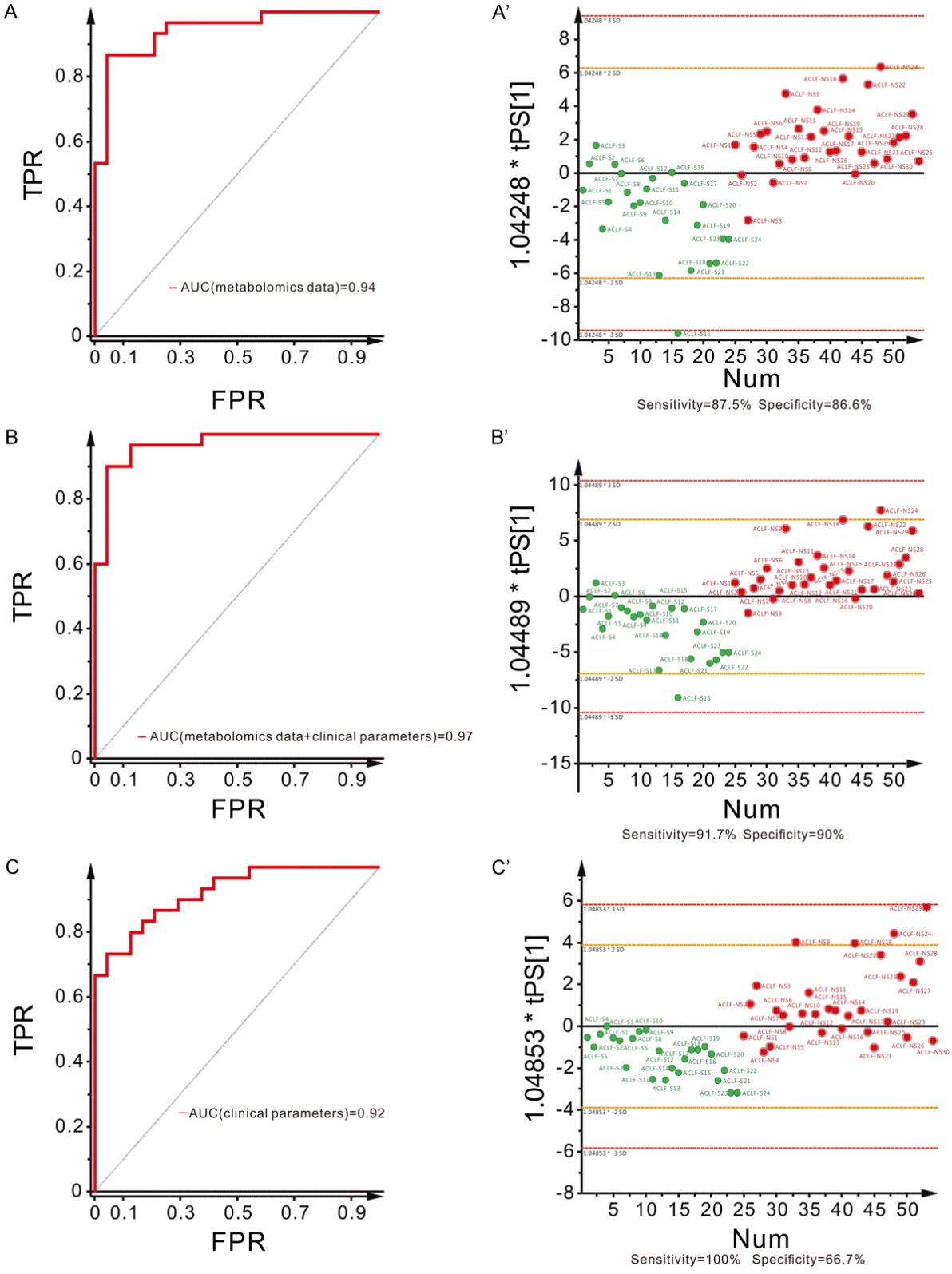
A
TPR
FPR
AUC(metabolomics data)=0.94
A'
1.04248 * tPS[1]
Num
Sensitivity=87.5% Specificity=86.6%
B
TPR
FPR
AUC(metabolomics data+clinical parameters)=0.97
B'
1.04489 * tPS[1]
Num
Sensitivity=91.7% Specificity=90%
C
TPR
FPR
AUC(clinical parameters)=0.92
C'
1.04853 * tPS[1]
Num
Sensitivity=100% Specificity=66.7%

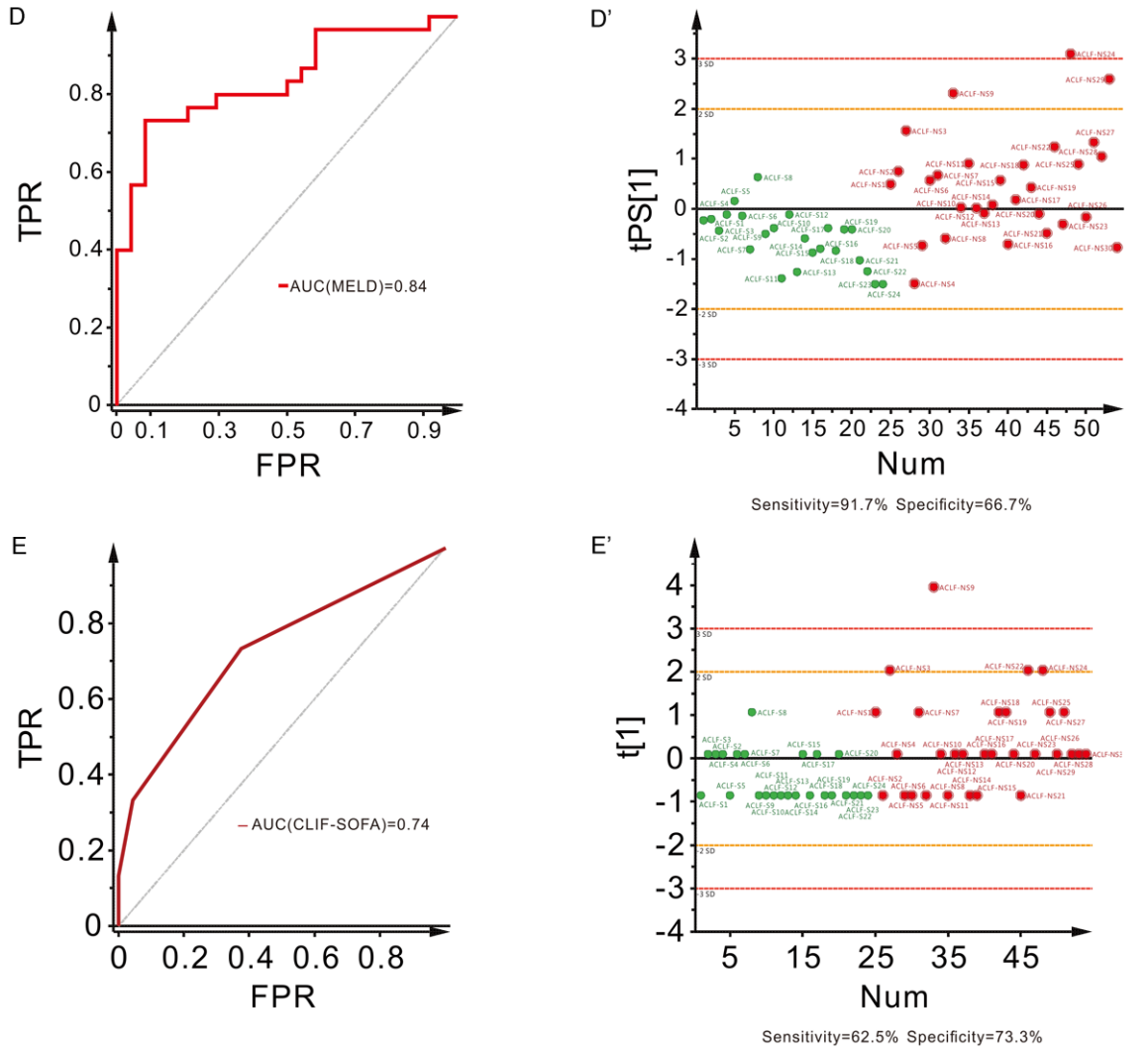

Figure 4. AUROC plots and predicted score plots derived from metabolomics data only (A, A'), metabolomics data plus clinical parameters (B, B'), clinical parameters only (C, C'), MELD scores only (D, D'), and CLIF-SOFA scores only (E, E').

(ACLF *vs.* CHB and ACLF-NS *vs.* ACLF-S). These fourteen metabolites, which might be closely related to the development of ACLF, belong to either amino acid metabolism pathways or lipid metabolism pathways. The detected changes of these fourteen metabolites and their potential roles in the progression of the ACLF disease are discussed in detail below.

Among the fourteen consecutively changed metabolites, twelve of them, including glutamine, methionine, valine, asparagine, leucine, isoleucine, betaine, threonine, tyrosine, 2-aminobutyrate, phenylalanine and glycine, are amino acids, indicating that amino acid metabolism plays a key role in the development and progression of HBV-ACLF. The liver is a key organ for amino acid (AA) metabolism, protein synthesis and protein breakdown. In fact, it has been shown that approximately 80% of the AAs absorbed from the digestive tract are depleted via amino acid and protein metabolism in the liver [19]. The striking upregulation of aromatic amino acids (AAAs), including tyrosine and phenylalanine, and two other amino acids, including methionine and betaine, in the serum samples of the ACLF patients, especially in the fatal cases, might be caused by the impaired hepatic metabolism and portosystemic shunting [20]. Under normal conditions, aromatic amino acids and methionine are mainly metabolized in the liver [21]. In the failing liver, the metabolic

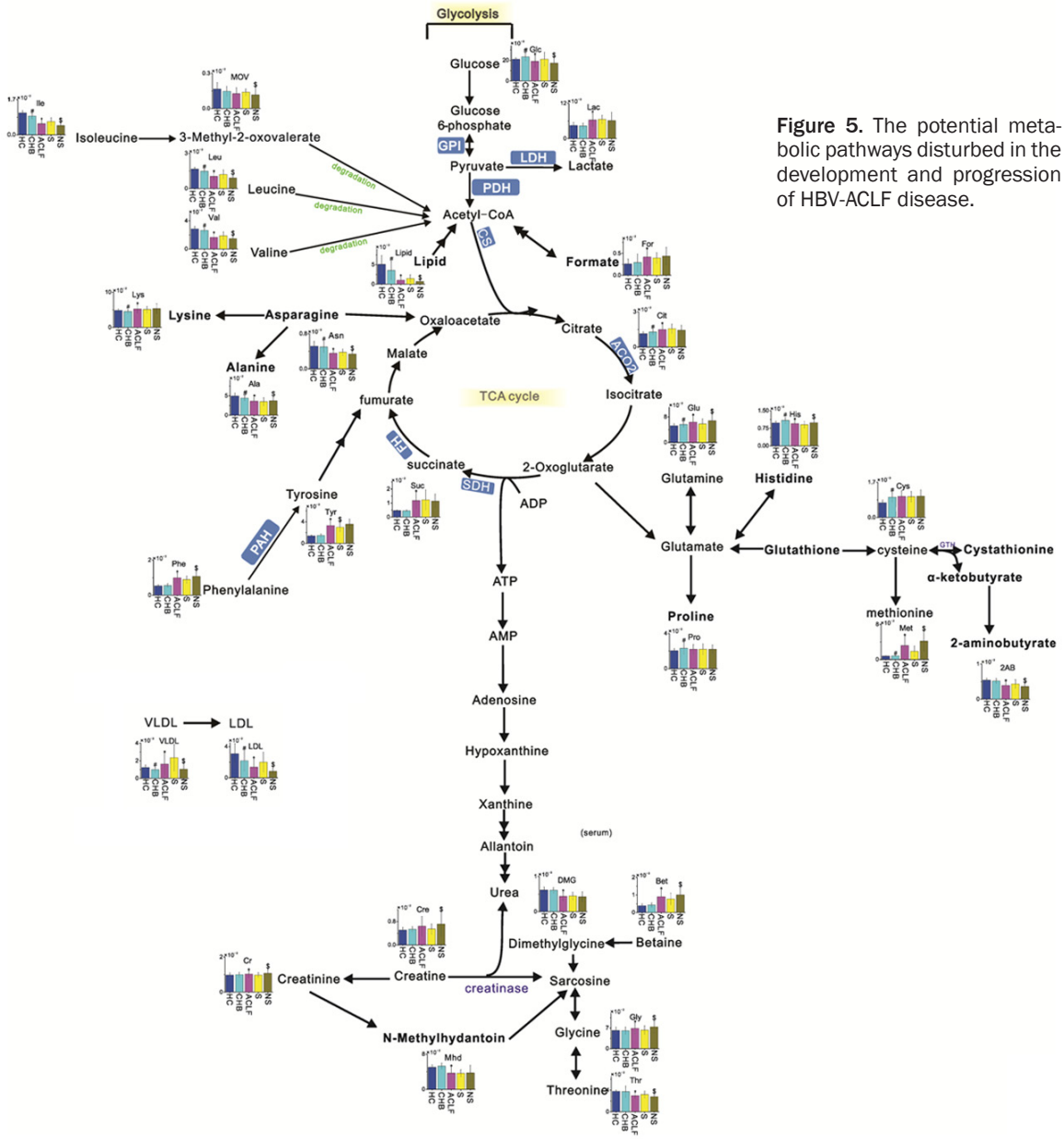

Figure 5. The potential metabolic pathways disturbed in the development and progression of HBV-ACLF disease.

enzymes of aromatic amino acids and methionine are defective, which then causes the accumulation of aromatic amino acids and methionine in serum [22]. Dejong *et al.* [23] suggested that aromatic amino acids might play critical roles in the pathogenesis of liver failure and hepatic encephalopathy. Elevated levels of serum tyrosine and phenylalanine have also been observed in NAFLF/NASH [24] and HCC patients [25]. Meanwhile, betaine, which is another strikingly upregulated metabolite in the ACLF patients, has been well known to play a key role in the control of hepatocellular hydration and hepatoprotection from different kinds of stress [26, 27]. Significant changes of betaine and methionine, which are two important components of the hepatic methylamine osmolyte metabolism pathway [26], are consistent with the severe hepatic damage induced by ACLF. Overall, the striking upregulation of tyrosine, phenylalanine, methionine and betaine in the serum samples of ACLF patients is intimately coupled to the development and progression of ACLF, and they might potentially serve as markers for the prognosis of ACLF.

Different from the aromatic amino acids, methionine and betaine, all three branched-chain

amino acids (BCAA), including valine, isoleucine and leucine, were significantly downregulated in the serum samples of the ACLF patients. Specifically, in comparison with the survivors, a greater decrease for these three amino acids was observed in the non-surviving ACLF patients (**Table 2**; **Figure 5**). Branched-chain amino acids are primarily catabolized in the skeletal muscle and kidney [28]. However, because BCAAs are the major energy source of amino acids, the observed decrease in ACLF patients might have been caused by the increased depletion of these amino acids by the extrahepatic tissues to compensate for the energy needs during liver insufficiency [20]. Advanced liver diseases are commonly accompanied by nutritional disturbances, which worsen the amino acid imbalance of the patients [29]. Consistent with the current knowledge, the consecutive accumulation of aromatic amino acids (tyrosine and phenylalanine) and the increasing breakdown of BCAAs were observed in the serum samples of the ACLF patients. This finding suggests that the BCAA/AAA ratio (the Fischer-ratio) could potentially serve as a prognostic marker for ACLF.

It has been reported that glutamine is an important index by which to judge the severity and the prognosis of liver failure. As reported by earlier studies, the elevated level of glutamine could be attributed to the disruption of the urea cycle [30]. Normally, the liver will promptly remove ammonia from the portal blood and produce urea through the urea cycle, but when hepatic failure occurs, the urea cycle will be hampered and some ammonia is fed to produce glutamine in the kidney and brain. In fact, a previous study showed that the magnitude of the increase of glutamine is significantly correlated with the severity of encephalopathy in patients with fulminant hepatic failure [31]. Laubenberger *et al.* [32] also revealed a significant correlation between the glutamine level in cerebrospinal fluid and the severity of encephalopathy in patients with decompensated liver cirrhosis. Consistent with the reported data, a consecutive upregulation of the intensity of glutamine signals in the serum samples of the CHB and ACLF patients was detected in our study, and more importantly, an additional increase of the glutamine level was observed in the non-surviving ACLF patients.

In addition to amino acid metabolism, our metabolomics data showed that the levels of serum lipid and LDL were consecutively downregulated upon the progression of ACLF. The decreases of the lipid and LDL levels in the serum of the ACLF patients could be potentially attributed to the loss of the lipid synthesis function of the liver induced by ACLF. It has been reported that lipids play an important role in the pathogenesis of liver fibrosis [12]. Our data indicate that the blood levels of lipids and LDL might be good indicators of liver function.

As mentioned above, the metabolomics data revealed that two groups of metabolites, including amino acids and lipids, play key roles in the development and progression of HBV-ACLF. These metabolites, especially the amino acids, could potentially serve as markers for the prognosis of this disease, and the serum BCAA/AAA ratio (the Fischer ratio) is linked to the prognosis of HBV-ACLF. Because the metabolic profiles of healthy controls, HBV carriers, HBV-ACLF non-survivors and HBV-ACLF survivors did show distinct characteristics, prognostic prediction models based on the metabolic profile data were then set up and evaluated (**Figure 4**). They clearly illustrate that the sensitivity and specificity of the predicted score plot of metabolomics data plus the clinical parameters reached the encouraging values of 91.7% and 90%, respectively. In sum, the abovementioned findings provide proof of concept that the global metabolic profiling data obtained from the NMR-based metabolomics analysis of the serum samples of ACLF patients is a reliable source to assess the severity and improve the accuracy of predicting the survival outcome of HBV-ACLF individuals at admission. This technique, when used in combination with other biochemical methods, could potentially offer ACLF patients a wider treatment window prior to transplantation.

However, given the relatively limited number of participants and analytical platforms used at present, further studies with larger prospective cohorts and multiple analytical techniques should be performed to confirm our metabolomic findings.

Acknowledgements

NMR data were acquired in the NMR facility of the Shanghai Institute of Materia Medica,

Chinese Academy of Sciences. This work was supported by the Ministry of Science and Technology of China major projects of the "12th Five-Year plan" (No. 2012ZX10005) and the science foundation for youth of Shanghai Municipal Health Bureau (No. 20134y011).

Disclosure of conflict of interest

None.

Authors' contribution

JW, NZ and ZQ designed the experiments. LJ, XL and NZ wrote the main manuscript text. YL, HZ, YZ, ZZ, HG, WY, ZQ and LJ collected the samples. XL acquired the NMR spectra. LJ and XL analyzed the data and prepared the figures and tables. All authors reviewed and agreed with the content of the manuscript.

Address correspondence to: Zhiping Qian and Jiefei Wang, Department of Liver Intensive Care Unit, Shanghai Public Health Clinical Center, Fudan University, Shanghai 201508, P. R. China. Tel: 86-21-37990333-3259; E-mail: zhipingqian@sina.com (ZPQ); wangjiefei@shaphc.org (JFW); Naixia Zhang, CAS Key Laboratory of Receptor Research, Department of Analytical Chemistry, Shanghai Institute of Materia Medica, Chinese Academy of Sciences, Shanghai 201508, P. R. China. Tel: 86-21-5080-6036; E-mail: nxzhang@simm.ac.cn

References

[1] Katoonizadeh A, Laleman W, Verslype C, Wilmer A, Maleux G, Roskams T and Nevens F. Early features of acute-on-chronic alcoholic liver failure: a prospective cohort study. Gut 2010; 59: 1561-1569.

[2] Shi KQ, Cai YJ, Lin Z, Dong JZ, Wu JM, Wang XD, Song M, Wang YQ and Chen YP. Development and validation of a prognostic nomogram for acute-on-chronic hepatitis B liver failure. J Gastroenterol Hepatol 2017; 32: 497-505.

[3] Graziadei IW. The clinical challenges of acute on chronic liver failure. Liver Int 2011; 31 Suppl 3: 24-26.

[4] Graziadei I. Liver transplantation organ allocation between Child and MELD. Wien Med Wochenschr 2006; 156: 410-415.

[5] Luo Y, Xu Y, Li M, Xie Y and Gong G. A new multiparameter integrated MELD model for prognosis of HBV-related acute-on-chronic liver failure. Medicine 2016; 95: e4696.

[6] Wiesner R, Edwards E, Freeman R, Harper A, Kim R, Kamath P, Kremers W, Lake J, Howard T, Merion RM, Wolfe RA and Krom R. Model for end-stage liver disease (MELD) and allocation of donor livers. Gastroenterology 2003; 124: 91-96.

[7] Pan HC, Jenq CC, Lee WC, Tsai MH, Fan PC, Chang CH, Chang MY, Tian YC, Hung CC, Fang JT, Yang CW and Chen YC. Scoring systems for predicting mortality after liver transplantation. PLoS One 2014; 9: e107138.

[8] Qu F, Zheng SJ, Liu S, Wu CS, Duan ZP and Zhang JL. Serum sphingolipids reflect the severity of chronic HBV infection and predict the mortality of HBV-acute-on-chronic liver failure. PLoS One 2014; 9: e104988.

[9] Ippolito JE, Xu J, Jain S, Moulder K, Mennerick S, Crowley JR, Townsend RR and Gordon JI. An integrated functional genomics and metabolomics approach for defining poor prognosis in human neuroendocrine cancers. Proc Natl Acad Sci U S A 2005; 28: 9901-9906.

[10] Clayton TA, Baker D, Lindon JC, Everett JR and Nicholson JK. Pharmacometabonomic identification of a significant host-microbiome metabolic interaction affecting human drug metabolism. Proc Natl Acad Sci U S A 2009; 25: 14728-14733.

[11] Wang JB, Pu SB, Sun Y, Li ZF, Niu M, Yan XZ, Zhao YL, Wang LF, Qin XM, Ma ZJ, Zhang YM, Li BS, Luo SQ, Gong M, Sun YQ, Zou ZS and Xiao XH. Metabolomic profiling of autoimmune hepatitis: the diagnostic utility of nuclear magnetic resonance spectroscopy. J Proteome Res 2014; [Epub ahead of print].

[12] Sands CJ, Guha IN, Kyriakides M, Wright M, Beckonert O, Holmes E, Rosenberg WM and Coen M. Metabolic phenotyping for enhanced mechanistic stratification of chronic hepatitis C-induced liver fibrosis. Am J Gastroenterol 2015; 110: 159-169.

[13] Qi SW, Tu ZG, Peng WJ, Wang LX, Ou-Yang X, Cai AJ and Dai Y. ^{1}H NMR-based serum metabolic profiling in compensated and decompensated cirrhosis. World J Gastroenterol 2012; 3: 285-290.

[14] Dabos KJ, Parkinson JA, Sadler IH, Plevris JN and Hayes PC. ^{1}H nuclear magnetic resonance spectroscopy-based metabonomic study in patients with cirrhosis and hepatic encephalopathy. World J Hepatol 2015; 7: 1701-1707.

[15] Lian J, Li X, Wang Y, Yang J, Liu W, Ma J, Chen D, Li L and Huang J. Metabolite variations between acute-on-chronic liver failure and chronic liver failure caused by hepatitis B virus based on ultra-performance liquid chromatography mass spectrometry. Biomed Pharmacother 2016; 84: 994-1000.

[16] Amathieu R, Nahon P, Triba M, Bouchemal N, Trinchet JC, Beaugrand M, Dhonneur G and Le Moyec L. Metabolomic approach by ^{1}H NMR

spectroscopy of serum for the assessment of chronic liver failure in patients with cirrhosis. J Proteome Res 2011; 10: 3239-3245.
[17] Saxena V, Gupta A, Nagana Gowda GA, Saxena R, Yachha SK and Khetrapal CL. ^{1}H NMR spectroscopy for the prediction of therapeutic outcome in patients with fulminant hepatic failure. NMR Biomed 2006; 19: 521-526.
[18] Liver Failure and Artificial Liver Group, Chinese Society of Infectious Diseases, Chinese Medical Association; Severe Liver Diseases and Artificial Liver Group, Chinese Society of Hepatology, Chinese Medical Association. Diagnostic and treatment guidelines for liver failure (2012 version). Zhonghua Gan Zang Bing Za Zhi 2013; 21: 177-183.
[19] Tsukada K, Moriyama T and Lieberman I. Liver amino acid pool may be homogeneous with respect to protein synthesis. J Biochem 1971; 70: 173-174.
[20] Morgan MY, Marshall AW, Milsom JP and Sherlock S. Plasma amino-acid patterns in liver disease. Gut 1982; 23: 362-370.
[21] Al Mardini H, Douglass A and Record C. Amino acid challenge in patients with cirrhosis and control subjects: ammonia, plasma amino acid and EEG changes. Metab Brain Dis 2006; 21: 1-10.
[22] Tessari P, Vettore M, Millioni R, Puricelli L and Orlando R. Effect of liver cirrhosis on phenylalanine and tyrosine metabolism. Curr Opin Clin Nutr Metab Care 2010; 13: 81-86.
[23] Dejong CH, van de Poll MC, Soeters PB, Jalan R and Olde Damink SW. Aromatic amino acid metabolism during liver failure. J Nutr 2007; 137: 1579S-1585S.
[24] Kalhan SC, Guo L, Edmison J, Dasarathy S, McCullough AJ, Hanson RW and Milburn M. Plasma metabolomic profile in nonalcoholic fatty liver disease. Metabolism 2011; 60: 404-413.
[25] Yang Y, Li C, Nie X, Feng X, Chen W, Yue Y, Tang H and Deng F. Metabonomic studies of human hepatocellular carcinoma using high-resolution magic-angle spinning ^{1}H NMR spectroscopy in conjunction with multivariate data analysis. J Proteome Res 2007; 6: 2605-2614.
[26] Hoffmann L, Brauers G, Gehrmann T, Häussinger D, Mayatepek E, Schliess F and Schwahn BC. Osmotic regulation of hepatic betaine metabolism. Am J Physiol Gastrointest Liver Physiol 2013; 304: G835-846.
[27] Schliess F and Haussinger D. The cellular hydration state: a critical determinant for cell death and survival. Biol Chem 2002; 383: 577-583.
[28] Holecek M. Relation between glutamine, branched-chain amino acids, and protein metabolism. Nutrition 2002; 18: 130-133.
[29] Tajiri K and Shimizu Y. Branched-chain amino acids in liver diseases. World J Gastroenterol 2013; 19: 7620-7629.
[30] Tripathi P, Bala L, Saxena R, Yachha SK, Roy R and Khetrapal CL. ^{1}H NMR spectroscopic study of blood serum for the assessment of liver function in liver transplant patients. J Gastrointestin Liver Dis 2009; 18: 329-336.
[31] Tofteng F, Hauerberg J, Hansen BA, Pedersen CB, Jorgensen L and Larsen FS. Persistent arterial hyperammonemia increases the concentration of glutamine and alanine in the brain and correlates with intracranial pressure in patients with fulminant hepatic failure. J Cereb Blood Flow Metab 2006; 26: 21-27.
[32] Laubenberger J, Haussinger D, Bayer S, Gufler H, Hennig J and Langer M. Proton magnetic resonance spectroscopy of the brain in symptomatic and asymptomatic patients with liver cirrhosis. Gastroenterology 1997; 112: 1610-1616.

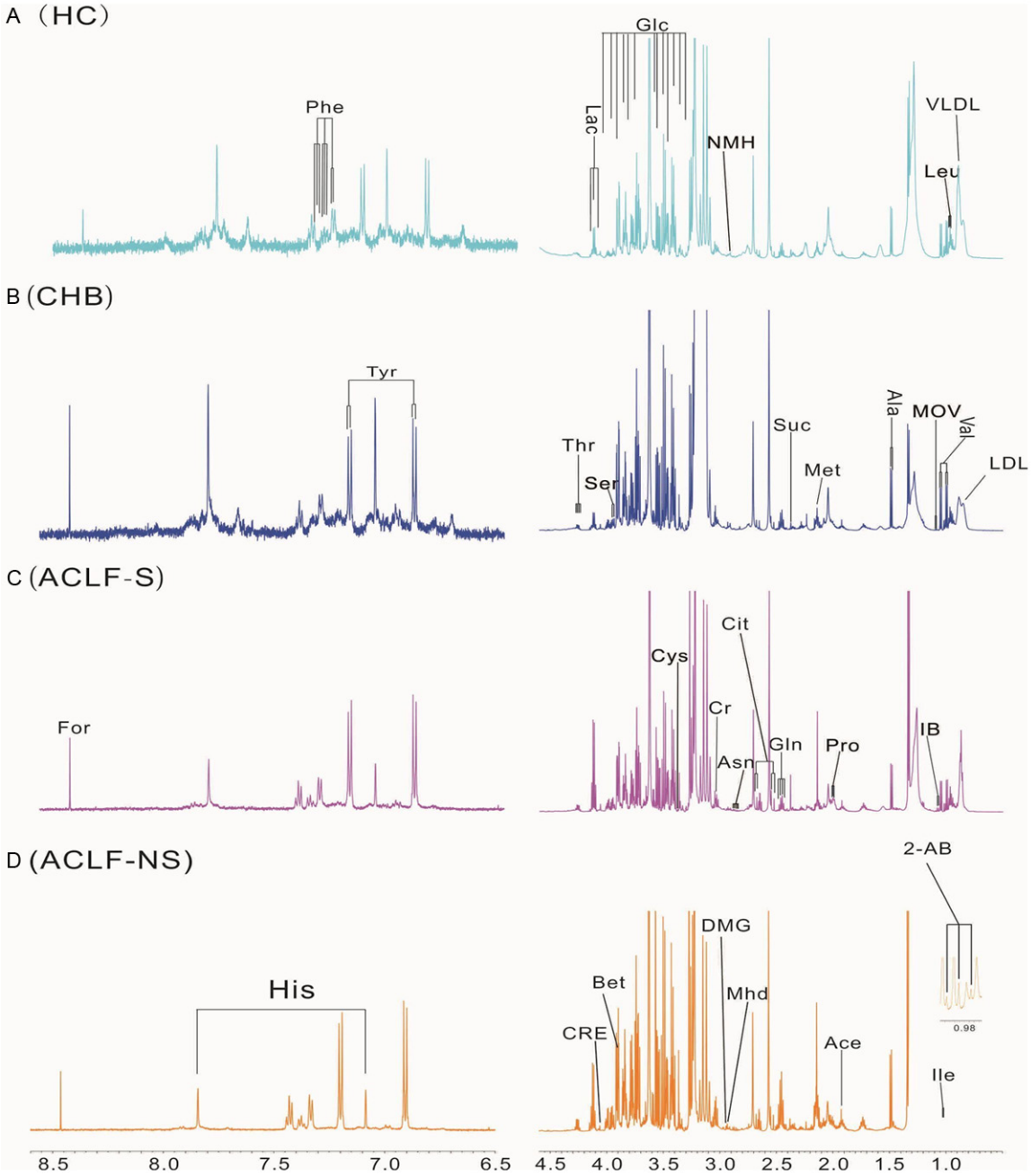

Figure S1. The 600-MHz ^{1}H NMR CPMG spectra (δ 0.9-4.7, δ 5.3-9.4) of serum samples obtained from the HC (A) group, the CHB (B) group, the ACLF-S subgroup (C), and the ACLF-NS subgroup (D). The abbreviations of the metabolites are defined in Table S1.

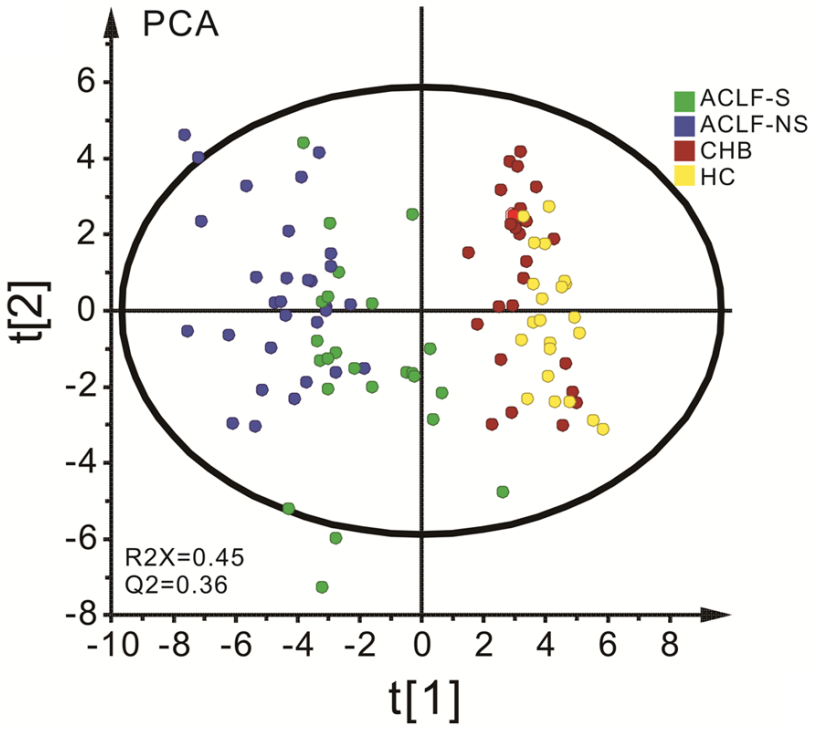

Figure S2. Score plot of PCA derived from ^{1}H NMR data of HC (●), CHB (●), ACLF-S (●), ACLF-NS (●) group samples.

Table S1. Resonance assignments of metabolites in ^{1}H NMR spectra

Metabolite (abbreviation)	Group	δ ^{1}H (ppm) (pH=7.4)#
Acetate (Ace)	CH3	1.93 (s)
Alanine (Ala)	α-CH	3.78 (q)
	β-CH_3	1.49 (d)
Asparagine (Asn)	α-CH	4.02 (dd)
	half β-CH_2	2.96 (dd)
	half β-CH_2	2.87 (dd)
Betaine (Bet)	α-CH_2	3.90 (s)
	N $(CH_3)_3$	3.27 (s)
Citrate (Cit)	half α-CH_2	2.55 (d)
	half α-CH_2	2.68 (d)
Creatine (Cr)	α-CH_2	3.95 (s)
	N-CH_3	3.04 (s)
Creatinine (CRE)	α-CH_2	4.03 (s)
	N-CH_3	3.05 (s)
Cysteine (Cys)	α-CH	3.97 (q)
	β-CH_2	3.06 (dd)
	β-CH_2	3.11 (dd)
Formate (For)	CH	8.46 (s)
Fumarate (FMA)	CH	6.52 (s)
Glutamine (Gln)	α-CH	3.78 (t)
	β-CH_2	2.44 (m)
	γ-CH_2	2.14 (m)
Glycine (Gly)	α-CH_2	3.57 (s)

Histidine (His)	α-CH	3.98 (dd)
	half β-CH_2	3.24 (dd)
	half β-CH_2	3.14 (dd)
	γ-CH_2	7.08 (s)
	CH	7.87 (s)
Isobutyrate (IB)	α-CH	2.49 (m)
	2×β-CH_3	1.06 (d)
Isoleucine (Ile)	α-CH	3.67 (d)
	β-CH	2.00 (m)
	γ-CH_3	1.01 (d)
	half γ-CH_2	1.42 (m)
	half γ-CH_2	1.21 (m)
	δ-CH_3	0.94 (t)
Lactate (Lac)	α-CH	4.13 (q)
	β-CH3	1.34 (d)
Low density lipoprotein (LDL)	CH_3	0.84 (bra)
	- $(CH_2)_n$-	1.25 (bra)
Leucine (Leu)	α-CH	3.73 (m)
	half β-CH_2	1.73 (m)
	half β-CH_2	1.70 (m)
	γ-CH	1.69 (m)
	δ-CH_3	0.97 (d)
	δ-CH_3	0.96 (d)
Lipid	CH3	0.93 (bra)
	- (CH2)n-	1.31 (bra)
	CH2-CH2-CO	1.68 (bra)
	CH2C=C	2.04 (bra)
	CH2-CO	2.23 (m)
	C=CCH2C=C, =CHCH2CH=CH	2.69 (bra)
	CH2CH2CH=	5.23 (bra)
Lysine (Lys)	α-CH	3.75 (t)
	β-CH_2	1.90 (m)
	half γ-CH_2	1.452 (m)
	half γ-CH_2	1.50 (m)
	δ-CH_2	1.72 (m)
	ε-CH_2	3.02 (t)
N, N-dimethylglycine (DMG)	α-CH_2	3.71 (s)
	N $(CH_3)_2$	2.93 (s)
N-methylhydantoin (Mhd)	α-CH	4.06 (s)
	CH_3	2.93 (s)
Methionine (Met)	α-CH	3.85 (q)
	β-CH_2	2.12 (m)
	γ-CH_2	2.22 (m)
	S-CH_3	2.11 (s)
Phenylalanine (Phe)	α-CH	7.33 (d)
	β-CH	7.43 (t)
	γ-CH	7.37 (t)
	half β-CH_2	3.98 (dd)
	half β-CH_2	3.27 (dd)
	α-CH	3.12 (dd)

Proline (Pro)	α-CH	4.14 (dd)
	half β-CH_2	2.36 (m)
	half β-CH_2	2.06 (m)
	half γ-CH_2	2.02 (m)
	half γ-CH_2	1.98 (m)
	half δ-CH_2	3.41 (m)
	half δ-CH_2	3.34 (m)
Succinate (Suc)	2×CH_2	2.40 (s)
Tyrosine (Tyr)		
Phenyl moiety:	α-CH	7.19 (d)
	β-CH	6.92 (d)
	half β-CH_2	3.05 (dd)
	half β-CH_2	3.19 (dd)
	α-CH	3.93 (dd)
Threonine (Thr)	α-CH	3.58 (d)
	β-CH	4.26 (m)
	γ-CH_3	1.35 (d)
Valine (Val)	α-CH	3.60 (d)
	β-CH	2.26 (m)
	γ-CH_3	1.05 (d)
	γ'-CH_3	0.99 (d)
Very low density lipoprotein (VLDL)	CH_3	0.87 (bra)
	-$(CH_2)_n$-	1.29 (bra)
2-Aminobutyrate (2-AB)	α-CH	3.70 (t)
	β-CH_2	1.90 (m)
	γ-CH_3	0.97 (t)
3-Methyl-2-oxovalerate (MOV)	α-CH	2.92 (m)
	half β-CH_2	1.68 (m)
	half β-CH_2	1.44 (m)
	γ-CH_3	0.88 (t)
	β-CH_3	1.07 (d)
α-Glucose (Glc)	^{1}CH	5.24 (d)
	^{2}CH	3.54 (dd)
	^{3}CH	3.71 (t)
	^{4}CH	3.40 (t)
	^{5}CH	3.82 (m)
	^{6}CH	3.84 (dd)
β-Glucose	^{1}CH	4.64 (d)
	^{2}CH	3.24 (dd)
	^{3}CH	3.49 (t)
	^{4}CH	3.38 (t)
	^{5}CH	3.45 (m)
	^{6}CH	3.89 (dd)

Note: #s, singlet; d, doublet; t, triplet; q, quartet; m, multiplet.